Cell-penetrating antimicrobial peptides – prospectives for targeting intracellular infections

Jesper S. Bahnsen[a], Henrik Franzyk[b], Edward J. Sayers[c], Arwyn T. Jones[c] and Hanne M. Nielsen[a].

[a]*Department of Pharmacy, Faculty of Health and Medical Sciences, University of Copenhagen, Universitetsparken 2, DK-2100 Copenhagen, Denmark.*

[b]*Department of Drug Design and Pharmacology, Faculty of Health and Medical Sciences, University of Copenhagen, Universitetsparken 2, DK-2100 Copenhagen, Denmark*

[c]*Cardiff School of Pharmacy and Pharmaceutical Sciences, Cardiff University, Cardiff, Wales, CF10 3NB, United Kingdom*

ABSTRACT

Purpose. To investigate the suitability of three antimicrobial peptides (AMPs) as cell-penetrating antimicrobial peptides.

Methods. Cellular uptake of three AMPs (PK-12-KKP, SA-3 and TPk) and a cell-penetrating peptide (penetratin), all 5(6)-carboxytetramethylrhodamine-labeled, were tested in HeLa WT cells and analyzed by flow cytometry and confocal microscopy. Furthermore, the effect of the peptides on eukaryotic cell viability as well as their antimicrobial effect were tested. In addition, the secondary structure and disrupting ability of the peptides in the presence of bilayer membranes of different composition were analyzed.

Results. AMP uptake relative to penetratin was ~13% (PK-12-KKP), ~66% (SA-3) and ~50% (TPk). All four peptides displayed a punctate uptake pattern in HeLa WT cells with co-localization to lysosomes and no indication that clathrin-mediated endocytosis was the predominant uptake mechanism. TPk showed the highest anti-bacterial activity. Only penetratin displayed clear secondary structure in the presence of membrane-mimicking liposomes. SA-3 exhibited selective disruption of liposomes mimicking Gram-positive and Gram-negative membranes.

Conclusion. PK-12-KKP is an unlikely candidate for targeting intracellular bacteria, as the eukaryotic cell-penetrating ability is poor. SA-3, affected the cellular viability to an unacceptable degree. TPk showed acceptable uptake efficiency, high antimicrobial activity and relatively low toxicity, and it is the best potential lead peptide for further development.

Key words: antimicrobial peptides; cell-penetrating peptides; antibiotics; *Staphylococcus aureus*; peptide-membrane interaction.

INTRODUCTION

Cell-penetrating peptides (CPPs) are short, often cationic peptides capable of internalizing into eukaryotic cells without damaging the plasma membrane at effective internalization concentrations, and therefore they are actively pursued as potential drug delivery vehicles [1]. Cationic antimicrobial peptides (AMPs) comprise a class of peptides structurally similar to cationic CPPs, and AMPs constitute an essential part of the innate immune system in almost all living organisms [2]. Most known AMPs exert their antibacterial effect via selective membrane disruption thereby killing the bacteria, but also intracellular targets have been identified for some AMPs (e.g. buforin II [3], drosocin [4] and apidaecin [5]). The two peptide classes, cationic CPPs and cationic AMPs, share features such as: (i) a relatively short chain length (10–40 residues), (ii) a positive net charge, important for initial interaction with phospholipid membranes possessing an overall negative charge, and (iii) an amino acid composition with a significant content of non-polar residues considered to promote their interaction with, and in the case of AMPs, insertion into the hydrophobic core of the membrane bilayer [6]. The dominant biological effect of such highly cationic peptides may be altered from cell-penetrating to antimicrobial or vice versa by even small modifications of their sequence. Thus, examples of successful development of both AMP-based CPPs (e.g. SynB1 [7] and Bac7 (15-24) [8]) and CPP-based AMPs (e.g. Pep-1-K) [9] have been reported. The increasing interest in the dual effects of these types of peptides has uncovered several examples of peptides exhibiting both eukaryotic cell membrane penetration and antimicrobial effects [10].

During the last decade, a massive increase in community-associated and nosocomial multidrug-resistant S*taphylococcus aureus* infections has been registered, now reaching an alarming level; combined with a high rate of recurrent infections this poses a serious healthcare problem [11]. Increasing evidence infers that the high incidence of recurrent infections is caused by bacteria internalizing into epithelial cells at the site of infection [12]. Thus, complete eradication is not obtainable through treatment with commonly applied antibiotics [13]. We propose that development of a suitable cell-penetrating antimicrobial peptide could provide an alternative treatment regime against such persistent intracellular infections either in itself or as part of a combination therapy. In a previous study [14], we found that the well-characterized CPP, penetratin and a number of its analogs in fact possess antimicrobial properties. In the present study, we investigated whether bacteria-penetrating AMPs could be applied as CPPs.

Zhu and coworkers [9] showed that modification via Gly → Lys substitution in the synthetic CPP, Pep-1, afforded a designed AMP, Pep-1-K (also denoted PK) that efficiently inhibited growth of both Gram-negative and Gram-positive bacteria. Further optimization towards a shorter analog was based on a 12 amino acid truncated version of PK with two lysine residues added to the C-terminus and three Thr→ Pro substitutions [15]. The resulting 14-mer PK-12-KKP displayed a more pronounced positive charge, low hydrophobicity, and only partial folding into a well-defined secondary structure due to the presence of the proline residues. Although the antimicrobial activity of PK and PK-12-KKP were comparable, their mode of action was indicated to be different as the latter exhibited a very low membrane depolarization of *S. aureus* similar to that of buforin 2 known to have an intracellular target. Joshi and coworkers [16] reported a range of synthetic peptides designed from an amphipathic template displaying mainly hydrophobic and cationic amino acids. Amongst these, a 12-mer peptide, SA-3 composed mainly of lysine and tryptophan, was found to exhibit efficient inhibition of both Gram-negative and Gram-positive bacteria as well as low hemolytic activity. Based on uptake of FITC-labeled peptide into *E. coli* and strong DNA binding properties of the peptide the authors suggested an internal target as the primary mode of action for SA-3 [16]. In addition, Zhu and co-workers reported that TPk, a peptidomimetic

analog of tritrpticin, displayed high activity against Gram-positive and Gram-negative bacteria as well as low cytotoxicity against eukaryotic cells [17]. The design of this analogue involved replacement of two proline residues with peptoid lysine residues (NLys), thereby increasing the overall molecular charge, while preserving the lack of amide protons required for hydrogen bonding to the backbone. Additionally, TPk depolarized the membrane potential of *S. aureus* to a low degree and only caused weak leakage of a fluorescent dye entrapped within negatively charged vesicles modeling the bacterial membrane. Confocal laser-scanning microscopy of bacteria exposed to FITC-labeled TPk showed clear accumulation of fluorescence in the cytoplasm, whereas the parent tritrpticin remained outside or associated to the cell membrane. These findings suggest that the mode of action for TPk involves inhibition of intracellular components after crossing the bacterial cell membrane.

The common feature of the three AMPs selected for this study is that investigations of their bacterial killing mechanism have inferred that they act via intracellular targets. By applying advanced artificial membrane systems to study these peptides, we expect to gain a more thorough understanding of their effects on the membranes of both bacteria and eukaryotic cells.

MATERIALS AND METHODS:

Materials

Reagents, resin and amino acid building blocks for solid-phase peptide synthesis were purchased from Iris Biotech (Merktredwitz, Germany) while DMF was acquired from VWR (Herlev, Denmark). Chemicals utilized were : 4-(2-hydroxyethyl)-1-piperazineethanesulfonic acid (HEPES) (AppliChem, Darmstadt, Germany), Hanks Balanced Salt Solution (HBSS) (Gibco, Paisley, UK), 3-(4,5-dimethylthiazol-2-yl)- 5-(3-carboxy-phenyl)-2-(4-sulphophenyl)-2H-tetrazolium (MTS) (Promega, Madison, WI, USA), phenazine methosulphate (PMS), sodium dodecyl sulfate (SDS), Eagle's minimal essential medium (EMEM), Triton X-100, calcein, diisopropylcarbodiimide (DIC), 1-hydroxybenzotriazole (HOBt), dimethylformamide (DMF) (all Sigma-

Aldrich, Buchs, Switzerland), 5(6)-carboxytetramethylrhodamine (TAMRA) (Fluka, Buchs, Switzerland), DRAQ7® (Biostatus, Leicestershire, UK), Dulbecco's Modified Eagle Medium (DMEM) (Invitrogen, Paisley, UK) and phosphate buffered saline (PBS) (Invitrogen, Paisley, UK) Sephadex G-100 (GE Healthcare, Little Chalfont, UK), 2,2,2-trifluoroethanol (TFE) (Acros organics, Geel, Belgium) Mueller Hinton Broth (MHB) (BD, Le Pont de Claix, France). The lipids: 1-palmitoyl-2-oleoyl-*sn*-glycero-3-phosphocholine (POPC), cholesterol, 1-palmitoyl-2-oleoyl-*sn*-glycero-3-phospho-(1'-rac-glycerol) (POPG), 1',3'-bis[1,2-dimyristoyl-*sn*-glycero-3-phospho]-*sn*-glycerol (Cardiolipin 14:0; CL), 1,2-dioleoyl-*sn*-glycero-3-phosphoethanolamine (DOPE) were obtained from Avanti Lipids, Alabaster AL, USA.

Methods

Solid phase peptide synthesis and labeling

Peptide synthesis was performed by Fmoc-based solid-phase peptide synthesis (SPPS) employing a microwave-assisted automated CEM Liberty synthesizer (CEM, Matthews, NC, USA); peptides were purified to >95% and 90% for TAMRA-labeled peptides as described earlier [14]. For the fluorophore labeling, TAMRA (2.5 equivalents) was used in a mixture of DIC (2.5 equivalents), and (HOBt; 2.5 equivalents) in (DMF) overnight at room temperature. The identity of the peptides was confirmed by HRMS spectra obtained by using a Bruker micrOTOF-Q II Quadropol MS detector; analyses were performed as ESI-MS (m/z): $[M + nH]^{n+}$ (Bruker, Bremen, Germany). An overview of the synthesis products can be found in Table I.

Cell culture

HeLa WT cells from the American Type Culture Collection (ATCC, Manassas, VA, USA) were maintained in EMEM supplemented with 10,000 IU/mL penicillin, 10 mg/mL streptomycin, 2 mM L-glutamine, 0.1 mM non-essential amino acids (all from Sigma-Aldrich, St. Louis, MO, USA), 1 mM sodium pyruvate (Invitrogen, Carlsbad, CA, USA), and 10% (v/v) fetal bovine serum (FBS) (Fisher Scientific, Waltham, MA, USA). Cells were kept under tissue culture conditions (5% CO_2, 37°C) and detached from culturing flasks at 80% confluency

by treatment with trypsin-EDTA, and subsequently subcultured once weekly. For the MTS/PMS assay HeLa WT cells were seeded at a density of ~30,000 cells/cm^2 in flat-bottomed 96-well Plates (Corning Costar, Sigma-Aldrich, Brøndby, Danmark). NIH 3T3 cells for MTS/PMS assay were acquired from ATCC (Manassas, VA, USA), maintained in DMEM supplemented with 10% (v/v) newborn calf serum (NCS) (Gibsco, Paisly, U.K.), 10,000 IU/mL penicillin, 10 mg/mL streptomycin and 2 mM L-glutamine and seeded in a flat-bottomed 96-well Plates (Corning Costar, Sigma-Aldrich, Brøndby, Danmark) at a density of ~69,000 cells/cm^2. HUVEC cells were acquired from the European Collection of Cell Cultures (ECACC) (Salisbury, U.K.) and maintained in Ham's F-12K (Kaighn's) medium supplemented with 10% (v/v) FCS, 0.1 mg/mL heparin, 0.03 mg/mL endothelial cell growth supplement as well as 10.000 IU/mL penicillin, 10 mg/mL streptomycin and 2 mM L-glutamine and seeded in a flat-bottomed 96-well Plates (Corning Costar, Sigma-Aldrich, Brøndby, Danmark) at a density of ~47,000 cells/cm^2. HeLa WT cells for confocal microscopy visualization were cultured on (poly-D-lysine)-coated, 35 mm imaging dishes (MatTek Glass Bottom Microwell Dishes, MatTek, Ashland, MA, USA) at a density of ~140,000 cells/cm^2 and for flow cytometry cells were seeded at a density of ~110,000 cells/cm^2 in 12-well plates (NUNC, Roskilde, Denmark). For all experiments, the cells were cultured for 22-24 h to obtain a subconfluent cell monolayer (confluency 80-90%).

MTS/PMS viability assay

The cells were washed twice with 37°C HBSS supplemented with 10 mM HEPES (hHBSS) and exposed to 100 µL of peptide solution in hHBSS (concentration range 1–256 µM) for 1 h under tissue culture conditions. A 0.2% (w/v) SDS solution and hHBSS were used as positive ($OD_{pos.ctrl}$) and negative ($OD_{neg.ctrl}$) control, respectively. The peptide solution was removed by inverting and gently tapping the back of the plate. Subsequently, a mixture of 240 µg/mL MTS and 2.4 µg/mL PMS in test buffer was applied. The plate was incubated shielded from light (37°C, 50 rpm) for approx. 2 h until the cells exposed to buffer (the negative control) reached an absorbance of ~1. Absorbance was measured on a POLARstar Optima (λ = 492 nm) (GMB Labtech, Offenburg, Germany). The relative cell viability (%) was calculated according to Eq. (1):

(1) Viability (%) = $(OD_{peptide} – OD_{pos.ctrl.}) / OD_{neg.ctrl.} – OD_{pos.ctrl.}$

Confocal laser-scanning microscopy (CLSM)

The cells were rinsed with DMEM supplemented with 10% (v/v) heat-inactivated fetal calf serum, 100 IU/mL penicillin and 100 µg/mL streptomycin (37°C). The medium was replaced with 200 µL of 10µM TAMRA–labeled peptide in PBS and incubated for 1 h under tissue culture conditions. Subsequently, the test solutions were discarded, the cells washed twice with DMEM, once with imaging medium (DMEM without phenol red), and finally resuspended in 300 µL of imaging medium containing 0.3% (v/v) DRAQ7®. Immediately hereafter, CLSM was performed using an inverted Leica SP5 confocal laser-scanning microscope (Leica Mikrosystems, Wetzlar, Germany) equipped with an Ar and HeNe laser and a 63× 1.4 NA oil immersion objective. Live-cell microscopy was performed at room temperature and with a fixed instrument configuration across all samples. Furthermore, endocytosis pathway markers: dextran and transferrin were applied: In lysosome labeling experiments the cells were incubated with 0.1 mg/mL 10 kDa dextran Alexa Fluor® 647 (Life Technologies, Basel, Switzerland) for 210 min, and the label subsequently chased into lysosomes via a further incubation in dextran-free medium for 20 h, after which the cells were incubated with peptide as described above. To investigate uptake by clathrin-mediated endocytosis, the cells were incubated for 50 min with 100 nM transferrin Alexa Fluor® 647 (Life Technologies, Basel, Switzerland), rinsed with Complete DMEM. PBS 100 nM transferrin Alexa Fluor® 647 was supplemented with TAMRA- peptides (200 µL) at various concentrations and incubated under tissue culture conditions for 10 min before proceeding with the washing and imaging procedure stated above.

Flow cytometry

Cellular internalization of TAMRA-labeled peptides was quantified by flow cytometry. Initially, the cells were washed once with 1 mL PBS (37°C), containing 10 µM peptide solution (700 µL in PBS) and incubated for 1 h

under tissue culture conditions. The cells were subsequently rinsed three times with ice-cold PBS. Detachment of the cells from the wells was done by addition of 0.01 % (w/v) trypsin-EDTA (200 µL, 10 min, 37°C, 5% CO_2), and after centrifugation (5 min, 1076 × g) the cells were washed twice with ice-cold PBS containing 10% (v/v) FBS. Lastly, the cells were resuspended in 500 µL PBS with 10% (v/v) FBS containing 0.3% (v/v) DRAQ7®. Flow cytometry analysis was performed shortly after the preparation by using a Gallios flow cytometer (Beckman Coulter, Fullerton, CA, USA). The fluorescence mean of 10,000 viable cells was recorded gating for forward and sideways scattering as well as for DRAQ7® fluorescence intensity.

Minimal inhibitory concentration (MIC)

The inhibitory effect of peptides on bacterial growth was determined by micro dilution broth assay according to Clinical Laboratory Standard Institute (CLSI) guidelines [19]. The peptides were assayed against *S. aureus* (ATCC 25923) and *E. coli* (ATCC 25922) in the dilution range 1-128 µM in MHB (experiments performed in triplicate on at least two separate days). The bacteria were inoculated to 5×10^5 CFU/mL and incubated at 35°C in ambient air for ~18 h, after which the MIC values were determined as the lowest concentration showing no visible growth as compared to the control without antibacterial compound added.

Liposome preparation

Liposomes were prepared by using a procedure previously described [14]. In brief, large unilamellar vesicles (LUV) were prepared from POPC and cholesterol in a molar ratio of 10:1 in order to mimic an eukaryotic cell membrane composition [20–22], while a liposome composition with POPG and synthetic CL in a molar ratio of 3:1 was used to mimic Gram-positive *S. aureus* membrane composition [20–22]. POPG, CL, and DOPE in a molar ratio of 2:7:1 were employed as a model for Gram-negative *Escherichia coli* membranes [20–22]. For liposomes, the lipid film was dispersed in Tris buffer (10 mM, pH 7.4), whereas calcein-loaded liposomes were formed in Tris buffer (10 mM, pH 7.4) containing 150 mM NaCl, 0.1 mM EDTA and 70 mM calcein. Excess calcein was removed by passing the liposomes through a Sephadex G-50 column.

Circular dichroism (CD) spectroscopy

CD spectra were measured as previously described [14]. In brief, peptide and liposomes were added to a quartz cell with 1 mm light path, and 5 consecutive scans were collected in the range 190–260 nm. The scans were averaged and the background contribution from buffer or liposome-containing buffer was subtracted. An Olis DSM 10 spectrophotometer (Olis, Bogart, GA, USA) was used for all measurements except the measurements with the POPG:CL:DOPE (2:7:1 molar ratio) which was performed on a J-815 CD spectrometer (Jasco, Easton, MD, USA).

Calcein release assay

To measure leakage from calcein-loaded liposomes, these were added to black 96-well plates (MicroWell 96 optical bottom plates, NUNC, Roskilde, Denmark) at a concentration of 1.2 μM lipid determined from the strongest fluorescent signal from the lysed calcein-containing vesicles in a volume of 180 μL. The fluorescence was monitored by utilizing a FLUOstar OPTIMA plate reader (GMB Labtech, Offenburg, Germany) at an excitation wavelength of 485 nm and an emission wavelength of 520 nm to determine $\mathbf{F_0}$. A volume of 20 μL of peptide solution was added and measurement of calcein leakage was initiated within 10 sec from the first addition of peptide, and the peptide-induced calcein leakage was recorded for a period of 680 sec (340 sec for PK-12-KKP with POPG/CL liposomes) in order to determine **F**. Subsequently, the liposomes were disrupted completely by addition of 20 μL 20% (v/v) Triton X-100, and then the signal from the total amount of calcein was recorded ($\mathbf{F_t}$). The relative release was calculated according to Eq. (2):

(2) $\text{Calcein leakage [\%]} = [(F-F_0)/(F_t-F)_0]\cdot 100\%$

Data analysis

Results are presented as the mean of three measurements ±SD, and unless otherwise stated experiments were performed in triplicate. Statistical significance was determined by the students *t*-test where $P<0.05$ is considered

significant. For the viability assays the 50% cellular viability (EC_{50}) was estimated by using Prism 6 for Mac OS X vs. 6.0 and by non-linear regression according to Eq. (3):

(3) Y = Bottom + (Top-Bottom)/(1 + (X/EC50)(-HillSlope)).

RESULTS

In the present study, three AMPs (PK-12-KKP, SA-3 and TPk) and a CPP (penetratin) were investigated with respect to their: (i) ability to internalize into eukaryotic cells, (ii) subcellular localization inside eukaryotic cells, (iii) ability to inhibit bacterial growth, (iv) influence on eukaryotic cell viability, and (v) interaction with different membrane models.

Uptake of short cationic AMPs and CPP in HeLa WT cells

To determine whether the three AMPs were capable of internalizing into eukaryotic cells, TAMRA-labeled variants of the peptides were used. The uptake efficiency of the three AMPs was compared to that of the similarly labeled well characterized CPP, penetratin. As expected, penetratin displayed a higher total cellular uptake as compared to the AMPs as determined by flow cytometry (Figure 1). The Pep-1 derived analog PK-12-KKP displayed a significantly lower uptake (~10% relative to penetratin) than the other compounds tested ($P<0.01$). SA-3 showed the highest uptake as compared to the other tested AMPs reaching a level of ~65% of the uptake of penetratin, which was significantly better than that of TPk ($P<0.05$). TPk exhibited intermediate uptake efficiency with about half the uptake found for penetratin.

Intracellular distribution and co-localization with endocytosis pathway markers

Microscopical analysis confirmed the flow cytometry data showing that the TAMRA-labeled variants of the AMPs and penetratin gave rise to significant uptake resulting in subcellular punctate distribution patterns

throughout the cytoplasm of the HeLa WT cells without affecting the viability of the cells (data not shown) as determined by addition of DRAQ7®; a DNA binding dye that selectively stains dead and permeabilized cells. Peptide uptake was also imaged in cells that first were stained with fluorescently labeled pulse/chased 10 kDa dextran that accumulates in lysosomes. As expected peptide incubations in lysosome-labelled cells for the four peptides gave rise to punctate fluorescent structures (Figure 2), and in the case of PK12-KKP and penetratin there was clear evidence of delivery to lysosomes manifested as co-localization with dextran fluorophore. Whether clathrin-dependent endocytosis of the peptides occurred to a significant extent was studied by testing in cells that were pre-incubated with fluorescent transferrin present in the media during these short peptide incubations. This resulted in an overall low uptake of PK-12-KKP with no discernible co-localization with transferrin suggesting that clathrin-mediated endocytosis is not utilized by the peptide. With respect to transferrin there was minimal co-localization with SA-3 and TPk, however, these cells also showed diffuse cytosolic staining. Penetratin localization was confined to punctate structures that did not overlap to any extent with transferrin. For all four peptides DRAQ7® positive cells were not observed indicating that at this 10 μM concentration the plasma membrane was not compromised to a degree that resulted in leakage of the dye to label nuclear DNA.

Cellular viability and antimicrobial effect

To assess the relative effects of the peptides on eukaryotic cell viability and bacterial growth, the results of the tetrazolium dye-based viability assay MTS/PMS and the determined minimal inhibitory concentration on *S. aureus* were compared. To gain insight regarding a possible selectivity of the peptides towards specific eukaryotic cells, the viability of HeLa WT cells as well as of fibroblast cells (NIH 3T3) and human umbilical vein endothelial cells (HUVEC) in the presence of the three AMPs and penetratin was investigated (Table II). No significant reduction in viability of all three cell lines upon exposure to PK-12-KKP was detected within the concentration range tested (i.e. up to 256 μM). By contrast, cell viability was severely lowered by SA-3 with EC_{50} values against HeLa WT and NIH 3T3 cell lines at concentrations 25-30 μM. HUVEC cells were generally

much less sensitive to the peptides, and SA-3 was the only peptide that affected these cells at the tested concentrations. TPk reduced the viability of HeLa WT cells with an EC_{50} value only slightly higher than that of SA-3, however, its cytotoxicity against NIH 3T3 cells was at least four times lower than that of SA-3. Also, for penetratin no significant decrease in cell viability of any of the cell lines was observed within the tested concentration range. Table II shows that overall, the antimicrobial activity of the AMPs was more pronounced towards the Gram-negative *E. coli* than against the Gram-positive *S. aureus*, and that TPk was the most effective AMP.

Membrane interactions

The folding behavior of the four peptides was examined by circular dichroism (CD) spectroscopy in the presence of liposomes at a peptide to lipid molar ratio of 1:100; a ratio that was previously used to successfully study CPP secondary structure in the presence of unilamellar vesicles [23]. Different liposome compositions were employed in order to investigate interactions with specific types of membranes. As a model for Gram-positive bacteria membranes POPG:CL liposomes at a molar ratio of 3:1 (70.0 nm, PdI < 0.1) was utilized, while for Gram-negative bacterial membranes POPG:CL:DOPE liposomes at a molar ratio of 2:7:1 (80.84 nm, PdI < 0.1), and for eukaryotic cell membranes POPC:cholesterol liposomes at a molar ratio of 10:1 (75.9 nm, PdI = 0.1), respectively, were employed.

The CD spectrum of the proline-rich PK-12-KKP (Figure 3a) displayed uncharacteristic spectra in the presence of all liposomal model membranes and in 90:10 (v/v) TFE-water, and thus no specific secondary structure of PK-12-KKP could be deduced. SA-3 appeared to possess some degree of α-helicity in 90% TFE with minima around 208 nm and 222 nm. The minimum at 222 nm was also observed in the presence of both POPG:CL and POPC:cholesterol liposomes, although it was more distinct for the latter. In the presence of both of these liposomal membrane variants, the 208 nm minimum flattens out (Figure 3b). TPk showed almost no variation in the secondary structure upon interaction with different liposomal model membranes as well as in 90% TFE. Due

to the small changes in the CD spectra, it was not possible to assign any change in specific secondary structure by analysis of the spectra obtained for TPk (Figure 3c). Penetratin exhibited a highly variable secondary structure depending on the different model membranes (Figure 3d). The CD spectrum of penetratin recorded in 90% TFE corresponds to a classical α-helix conformation with minima at 208 nm and 222 nm along with a positive ellipticity in the range below 200 nm. In the presence of POPG:CL liposomes, penetratin seems to adopt an antiparallel β-sheet-like secondary structure with a minimum just below 220 nm and a maximum around 200 nm, while in the presence of the POPG:CL:DOPE liposomes no unambiguous secondary structure was observed. However, in the presence of POPC:cholesterol liposomes penetratin remained unstructured.

Calcein-containing liposomes of the same compositions as described above were exposed to varying peptide concentrations and the change in fluorescence over time was measured in order to assess both the degree and the kinetics of the membrane disruption induced by the peptides. The liposomes prepared with calcein displayed monomodal size distributions, yet overall they displayed a slightly smaller size than the ones without calcein; namely POPG:CL (molar ratio 3:1, 48.8 nm, PdI = 0.3), POPG:CL:DOPE (molar ratio 2:7:1, 51.6 nm, PdI = 0.2) and POPC:cholesterol (molar ratio 10:1, 39.1 nm, PdI < 0.1). When comparing the specific model membranes, clear differences were found regarding the maximal amount of calcein released upon exposure to the three peptides for up to 680 sec (Table III). Considering the individual peptides, PK-12-PPK gave rise to a low partial calcein leakage of 13-25 % for all three liposomal compositions. Overall, SA-3 resulted in a higher relative leakage, but with a higher degree of selectivity towards the liposomes modeling the bacterial membranes. Thus, SA-3 induced a high relative leakage (82% to completion) from the bacteria-mimicking liposomes, whereas the eukaryotic model liposomes only released 33% of the encapsulated calcein at the same peptide concentration. TPk had only a minimal effect on the POPG:CL:DOPE (2:7:1) liposomes mimicking the *E. coli* membrane as only ~3% of the calcein was released. In contrast, TPk disrupted both POPG:CL (3:1) liposomes mimicking *S. aureus* membranes and liposomes corresponding to a mammalian membrane composition releasing more than

30% of the encapsulated calcein. Penetratin exhibited a selective disruption of the *S. aureus* model liposomes with low disruptive capacity for the other two liposome compositions.

More detailed insight into the effects of SA-3 and penetratin on the different model membranes was gained by depicting comparative time-resolved and concentration-dependent profiles (Figure 4). The release of calcein from POPG:CL liposomes triggered by SA-3 is immediate, as the first measurement in the presence of 1.6 μM peptide showed ~20% calcein release (Figure 4). For penetratin, a slow initial calcein release was observed with a lag period of 40 sec, however, after 10 min full liposomal disruption was observed, while SA-3 reached a total release of 82%. Inspection of the concentration-dependent release of calcein from the POPG:CL model membranes revealed that these vesicles are more sensitive to penetratin than to SA-3 over the entire concentration range, even though the initial release rate is more rapid for SA-3.

DISCUSSION

The peptides investigated in this study have previously been tested for their antibacterial activity [15–17], whereas the objective of the current study was to assess their potential to target bacteria internalized in eukaryotic host cells. Quantification of the cellular uptake of the peptides allowed a ranking of these sequences according to their internalization efficiency in comparison to that of penetratin, a well-characterized CPP that has previously been shown to internalize efficiently into several eukaryotic cell lines [24,25] including HeLa WT cells [26]. Further, the distribution pattern of the AMPs in HeLa WT cells was assayed by confocal microscopy with and without fluorophore-labeled dextran as an endocytic probe that can be used to label the entire endolysosomal pathway or specifically lysosomes [27], which under the applied experimental conditions accumulate in the late vacuolar system, particularly in the lysosomes. Fluorophore-labeled transferrin known to be taken up by clathrin-dependent endocytosis [28] was included to investigate a potential contribution to the uptake via this pathway. Expectedly, penetratin showed a punctate uptake pattern with some co-localization with

dextran, and no or poor co-localization with transferrin indicating that its uptake is not receptor-mediated. This confirms earlier reports supporting a non-receptor mediated endocytosis of penetratin [29]. Although reports have indicated that direct translocation [30] or clathrin-dependent endocytosis are responsible for penetratin uptake [31], this was not evident under the conditions applied in the present study. It has also been debated that penetratin uptake most likely involves a combination of direct translocation and endocytotic pathways, while the dominant mechanism seems to be highly dependent on the specific experimental conditions [32].

The secondary structure of the peptides in the presence of three different liposomal compositions was examined by CD spectroscopy. Penetratin showed a classical α-helical conformation in TFE-water 90:10, but in the presence of POPG:CL:DOPE (molar ratio 2:7:1) liposomes mimicking the membrane of *E. coli* it did not show any clear secondary structure, however, its CD spectrum might represent a mix of partial α-helix and β-sheet conformations. To determine the influence of the peptides on immediate cell toxicity [8], various cell lines were exposed to the peptides, and their viability determined. Penetratin showed no impact on cell viability within the tested concentration range in accordance with our earlier findings [14]. A general trend was that HeLa WT cells were more sensitive towards the tested compounds as compared to the HUVEC and NIH 3T3 cells. This is in accordance with earlier observations on the membrane toxicity of short cationic AMP mimics towards various cell lines [33].

The propensity of penetratin to adopt an α-helical conformation while interacting with membranes mimicking eukaryotic cells was very low in disagreement with earlier findings [14]. This confirms that the presence of POPG is important for induction of secondary structure in penetratin corroborating earlier studies demonstrating that unstructured penetratin conformations are predominant in the presence of purely PC-based lipid systems [22]. To test the effect of the peptides on the integrity of different model membranes the corresponding liposomes containing a self-quenching solution of calcein were prepared and exposed to the AMPs and CPP. Penetratin showed negligible calcein release from the model liposomes mimicking eukaryotes and *E. coli* (8% and 13% release, respectively), whereas complete disruption of the liposomes mimicking *S. aureus* membranes

indicated selectivity toward this membrane model composition. Interestingly, in the bacterial inhibition assay, penetratin showed a stronger inhibition of *E. coli* than of *S. aureus*, indicating a mode of action against *E. coli* other than simple membrane disruption. The MIC values were within the range of earlier findings for penetratin [14,34–36].

Surprisingly, the amount of PK-12-KKP taken up by HeLa WT cells was significantly less than that seen for penetratin even though its design is based on a CPP template. Apparently, the modifications of the CPP aimed at conferring antimicrobial properties to the analogue concomitantly reduced its capability for eukaryotic internalization. Visualization of cell uptake by confocal microscopy showed that despite relatively low internalization of PK-12-KKP, some intracellular presence was clearly detectable. The peptide exhibited a punctate uptake pattern that showed some co-localization with internalized dextran, indicating uptake by endocytosis and trafficking of the peptide to the late stages of the endocytic pathway. No co-localization with transferrin was observed, suggesting that uptake is not mediated via clathrin-coated endocytosis. To understand the initial peptide-membrane interaction, PK-12-KKP was investigated by CD spectroscopy in the presence of the three different model membranes, and the spectra of the peptide in all cases indicated a very high presence of unstructured conformations confirming earlier studies done in SDS micelles [15]. Since secondary structure (e.g. α-helical folding) often has been shown to be a prerequisite for efficient CPP uptake [37,38], the primarily unstructured conformation of PK-12KKP is a plausible cause of its low uptake. Exposure of mammalian cells to PK-12-KKP only gave rise to a minor negative effect on their viability indicating low affinity for eukaryotic membranes in accordance with its low propensity for internalization. Interestingly, induction of dye leakage from the calcein-containing liposomes by PK-12-KKP only differed slightly between the three liposomal compositions implying a lack of bacteria-specific membrane disruption. Despite this fact, the potency of PK-12-KKP was modest (MIC of 32 μM and 16-32 μM against *S. aureus* and *E. coli*, respectively) deviating significantly from an earlier investigation of its antimicrobial activity with a MIC of 2 μM against both *S. aureus* (KCTC 1621) and *E. coli* (KCTC 1682) tested in a low-nutrition 1% (w/v) peptone solution [15], which has been

shown to drastically diminish bacterial survivability [39]. However, as the present MIC determinations were performed in MHB according to CLSI recommendations [19], this may explain the observed discrepancies. Overall, the low uptake of PK-12-KKP into eukaryotic cells combined with a modest antibacterial activity do not favor a potential application in targeting intracellular bacteria.

SA-3 is a synthetic designed AMP that showed the highest cellular uptake of the three investigated AMPs, most likely due to its high content of both cationic and hydrophobic residues; this feature is known to facilitate CPP uptake [40]. Furthermore, the peptide displays a slight propensity for adopting an α-helical secondary structure that also may promote cellular internalization. The intracellular distribution of SA-3 was punctate, and thus similar to that seen for penetratin and PK-12-KKP. Also for this AMP, co-localization with markers of the endocytotic pathway indicated an uptake mechanism distinct from that utilized by transferrin. A small increase in peptide concentration would likely have revealed DRAQ7® positive cells as concentrations used for microscopy were close to that showing toxicity using the MTS/PMS assay for this peptide. This was the most toxic peptide against eukaryotic cells, however, the antimicrobial potency of this peptide are in the same range as PK-12-KKP (*E. coli* 16-32 μM; *S. aureus* 32 μM), which is significantly lower than reported in literature (i.e. MICs of 1.2 μM and 0.6 μM for *S. aureus* and *E. coli*, respectively), however, different strains were tested [16]. The effect of the two peptides, PK-12-KKP and SA-3, on the viability of NIH 3T3 cells and HeLa WT cells were almost equal. When interacting with calcein-containing liposomes SA-3 completely disrupted those mimicking *E. coli* membranes, while the liposomes mimicking *S. aureus* membranes released ~80% of the encapsulated calcein. By contrast, SA-3 induced only ~33% disruption of the liposomes mimicking eukaryotic membranes. Thus, despite a relatively high release, this indicates that SA-3 displays some degree of selectivity towards bacterial membrane compositions. Comparison of the calcein release kinetics of SA-3 interacting with liposomes mimicking *S. aureus* with that of penetratin revealed an immediate onset of membrane disruption, with a critical concentration of SA-3 of ~0.1 μM, in contrast to the slower release triggered by penetratin. While SA-3 shows capacity for eukaryotic internalization its significant effect on cellular viability is problematic in relation to a

potential use against internalized bacteria. Nevertheless, the indication of secondary structure and its apparent selectivity towards bacterial membranes suggest that SA-3 may constitute a useful design template allowing for optimization of cellular uptake over cytotoxicity.

The peptidomimetic tritrpticin analog TPk exhibited ~50% uptake efficiency compared to penetratin and slightly lower than that of SA-3. The relatively high uptake of TPk is likely a result of its high content of cationic and non-polar amino acids. The intracellular localization of this peptidomimetic was marginally more pervasive than seen for the other peptides. However, there was still a clear punctate intracellular distribution, but with significantly less co-localization with dextran as compared to that observed for the other peptides. This could indicate that TPk is trafficked to a different subcellular localization or that there is loss of peptide into the cytosol via endosomal escape. No clear secondary structure was apparent from the CD spectra of TPk. The antimicrobial activity of TPk was up to 4-fold higher than that of the other tested AMPs. However, these MIC values are higher than what was reported in the literature, by Zhu and coworkers [17] who determined inhibitory concentrations of 2 μM for *E. coli* (KCTC 1682) and 1 μM for *S. aureus* (KCTC 1261) in a 1% (w/v) peptone solution. Surprisingly, TPk only gave rise to a minor calcein leakage when tested at 1.6 μM on the membrane model of *S. aureus*, releasing 32.5% of the encapsulated calcein, which is less than the release induced by both SA-3 ($P<0.001$) and penetratin ($P<0.001$), and only slightly higher than that of PK-12-PPK ($P<0.001$). From the liposomes mimicking *E. coli* membranes only 2.7% calcein were released, and the peptide was thus practically inactive towards this membrane model, while the *in vitro* antibacterial activity was pronounced. This confirms that the antibacterial effects do not rely exclusively on membrane disruption involving phospholipids. The interaction of TPk with the eukaryotic membrane model gave results comparable to those of the other AMPs. Moreover, TPk had a less negative effect on the viability of the three cell lines as compared to SA-3, but overall it was more membrane-disrupting than PK-12-KKP and penetratin. Zhu and coworkers reported an EC_{50} value >100 μM for TPk when assayed for viability of both HeLa and NIH 3T3 cells as determined by the MTT assay [17], which is in agreement with our findings for NIH 3T3 cells, but somewhat higher than the 41 μM towards

HeLa cells found in the present study. The intermediate uptake efficiency and notable effect on viability are less desirable for this peptide as a lead candidate aiming at targeting intracellular infections, but a high antimicrobial effect and enhanced selectivity increases its potential value as a template for further optimization.

CONCLUSION

In summary, the present study reports on the applicability of three different AMPs for targeting intracellular infections. Thus, the peptides were ranked against the well-known CPP penetratin with respect to cellular uptake and distribution. Also, their effect on eukaryotic and prokaryotic cell viability and leakage-inducing effect on liposomal membranes was compared. It was shown that the uptake mechanism for all tested peptides is very unlikely to involve clathrin-mediated endocytosis, and that they all aside from TPk are trafficked to lysosomes. Furthermore, TPk showed a stronger inhibitory effect on both Gram-positive and Gram-negative bacteria as compared to the other tested AMPs. One of the peptides, SA-3 reported to have an intracellular target, exhibited potent disrupting effects on bacteria-mimicking membranes of both Gram-positive and Gram-negative bacteria. PK-12-KKP was found to be well tolerated in eukaryotic cell models and with good antimicrobial properties, however, with weak eukaryotic internalization ability. Based on these investigations, TPk appears to be the best candidate for further investigations as an AMP capable of targeting intracellular infections as it may potentially be optimized for cell-penetration yielding an effective tool for eradication of bacteria residing inside epithelial cells.

ACKNOWLEDGEMENTS

The authors would like to thank Karina Juul Vissing, Maria Læssøe Pedersen, Thara Qais Hussein, Fabrice Rose and Uraiwan Adamsen for excellent technical assistance, Associate Professor Peter W. Thulstrup for use of CD

spectrometer, Kenneth Johansen for performing HRMS (all from University of Copenhagen) and Statens Serum Institut, CPH Denmark for providing bacterial strains for testing. We acknowledge Brødrene Hartmanns Fond, Danish Agency for Science Technology and Innovation (DanCARD, grant no. 06-097075), The Alfred Benzon Foundation and Drug Research Academy for financial support.

REFERENCES

1. Patel LN, Zaro JL, Shen W-C. Cell penetrating peptides: intracellular pathways and pharmaceutical perspectives. Pharm Res. 2007;24(11):1977–1992.

2. Zasloff M. Antimicrobial peptides of multicellular organisms. Nature. 2002;415(6870):389–395.

3. Park CB, Kim HS, Kim SC. Mechanism of action of the antimicrobial peptide buforin II: buforin II kills microorganisms by penetrating the cell membrane and inhibiting cellular functions. Biochem Biophys Res Commun. 1998;244(1):253–257.

4. Otvos L, O I, Rogers ME, Consolvo PJ, Condie BA, Lovas S, Bulet P, Blaszczyk-Thurin M. Interaction between heat shock proteins and antimicrobial peptides. Biochemistry. 2000;39(46):14150–14159.

5. Castle M, Nazarian A, Yi SS, Tempst P. Lethal effects of apidaecin on Escherichia coli involve sequential molecular interactions with diverse targets. J Biol Chem. 1999;274(46):32555–32564.

6. Almeida PF, Pokorny A. Mechanisms of antimicrobial, cytolytic, and cell-penetrating peptides: from kinetics to thermodynamics. Biochemistry. 2009;48(34):8083–8093.

7. Rousselle C, Clair P, Lefauconnier JM, Kaczorek M, Scherrmann JM, Temsamani J. New advances in the transport of doxorubicin through the blood-brain barrier by a peptide vector-mediated strategy. Mol Pharmacol. 2000;57(4):679–686.

8. Sadler K, Eom K, Yang J, Dimitrova Y. Translocating proline-rich peptides from the antimicrobial peptide bactenecin 7. Biochemistry. 2002;41(48):14150–14157.

9. Zhu WL, Lan H, Park I-S, Kim J Il, Jin HZ, Hahm K-S, Shin SY. Design and mechanism of action of a novel bacteria-selective antimicrobial peptide from the cell-penetrating peptide Pep-1. Biochem Biophys Res Commun. 2006;349(2):769–774.

10. Splith K, Neundorf I. Antimicrobial peptides with cell-penetrating peptide properties and vice versa. Eur Biophys J. 2011;40(4):387–397.

11. Boucher HW, Corey GR. Epidemiology of methicillin-resistant Staphylococcus aureus. Clin Infect Dis. 2008;46 Suppl 5:S344–S349.

12. Garzoni C, Kelley WL. Staphylococcus aureus: new evidence for intracellular persistence. Trends Microbiol. 2009;17(2):59–65.

13. Clement S, Vaudaux P, Francois P, Schrenzel J, Huggler E, Kampf S, Chaponnier C, Lew D, Lacroix J-S. Evidence of an intracellular reservoir in the nasal mucosa of patients with recurrent Staphylococcus aureus rhinosinusitis. J Infect Dis. 2005;192(6):1023–1028.

14. Bahnsen JS, Franzyk H, Sandberg-Schaal A, Nielsen HM. Antimicrobial and cell-penetrating properties of penetratin analogs: Effect of sequence and secondary structure. Biochim Biophys Acta. 2012;1828(2):223–232.

15. Zhu WL, Hahm K-S, Shin SY. Cell selectivity and mechanism of action of short antimicrobial peptides designed from the cell-penetrating peptide Pep-1. J Pept Sci. 2009;15(9):569–575.

16. Joshi S, Bisht GS, Rawat DS, Kumar A, Kumar R, Maiti S, Pasha S. Interaction studies of novel cell selective antimicrobial peptides with model membranes and E. coli ATCC 11775. Biochim Biophys Acta. 2010;1798(10):1864–1875.

17. Zhu WL, Lan H, Park Y, Yang S-T, Kim J Il, Park I-S, You HJ, Lee JS, Park YS, Kim Y, Hahm K-S, Shin SY. Effects of Pro --> peptoid residue substitution on cell selectivity and mechanism of antibacterial action of tritrpticin-amide antimicrobial peptide. Biochemistry. 2006;45(43):13007–13017.

18. Derossi D, Joliot a H, Chassaing G, Prochiantz A. The third helix of the Antennapedia homeodomain translocates through biological membranes. J Biol Chem. 1994;269(14):10444–10450.

19. CLSI. Methods for Dilution Antimicrobial Susceptibility Tests for Bacteria That Grow Aerobically• ; Approved Standard — Ninth Edition. CLSI document M07-A9. Wayne, PA: Clinical and Laboratory Standards Institute; 2012.

20. Bi X, Wang C, Ma L, Sun Y, Shang D. Investigation of the role of tryptophan residues in cationic antimicrobial peptides to determine the mechanism of antimicrobial action. J Appl Microbiol. 2013;115(3):663–672.

21. Epand RF, Schmitt MA, Gellman SH, Epand RM. Role of membrane lipids in the mechanism of bacterial species selective toxicity by two alpha/beta-antimicrobial peptides. Biochim Biophys Acta. 2006;1758(9):1343–1350.

22. Ishibashi J, Saido-Sakanaka H, Yang J, Sagisaka A, Yamakawa M. Purification, cDNA cloning and modification of a defensin from the coconut rhinoceros beetle, Oryctes rhinoceros. Eur J Biochem. 1999;266(2):616–623.

23. Magzoub M, Eriksson LEG, Gräslund A. Comparison of the interaction, positioning, structure induction and membrane perturbation of cell-penetrating peptides and non-translocating variants with phospholipid vesicles. Biophys Chem. 2003;103(3):271–288.

24. Thoren P. Uptake of analogs of penetratin, Tat(48-60) and oligoarginine in live cells. Biochem Biophys Res Commun. 2003;307(1):100–107.

25. Tréhin R, Krauss U, Beck-Sickinger AG, Merkle HP, Nielsen HM. Cellular uptake but low permeation of human calcitonin-derived cell penetrating peptides and Tat(47-57) through well-differentiated epithelial models. Pharm Res. 2004;21(7):1248–1256.

26. Letoha T, Gaál S, Somlai C, Venkei Z, Glavinas H, Kusz E, Duda E, Czajlik A, Peták F, Penke B. Investigation of penetratin peptides. Part 2. In vitro uptake of penetratin and two of its derivatives. J Pept Sci. 2005;11(12):805–811.

27. Al-Taei S, Penning NA, Simpson JC, Futaki S, Takeuchi T, Nakase I, Jones AT. Intracellular traffic and fate of protein transduction domains HIV-1 TAT peptide and octaarginine. Implications for their utilization as drug delivery vectors. Bioconjug Chem. 2006;17(1):90–100.

28. Al Soraj M, He L, Peynshaert K, Cousaert J, Vercauteren D, Braeckmans K, De Smedt SC, Jones AT. siRNA and pharmacological inhibition of endocytic pathways to characterize the differential role of macropinocytosis and the actin cytoskeleton on cellular uptake of dextran and cationic cell penetrating peptides octaarginine (R8) and HIV-Tat. J Control Release. 2012;161(1):132–141.

29. Jones SW, Christison R, Bundell K, Voyce CJ, Brockbank SM V, Newham P, Lindsay MA. Characterisation of cell-penetrating peptide-mediated peptide delivery. Br J Pharmacol. 2005;145(8):1093–1102.

30. Alves ID, Bechara C, Walrant A, Zaltsman Y, Jiao C-Y, Sagan S. Relationships between Membrane Binding, Affinity and Cell Internalization Efficacy of a Cell-Penetrating Peptide: Penetratin as a Case Study. Gasset M, editor. PLoS One. 2011;6(9):e24096.

31. Duchardt F, Fotin-Mleczek M, Schwarz H, Fischer R, Brock R. A comprehensive model for the cellular uptake of cationic cell-penetrating peptides. Traffic. 2007;8(7):848–866.

32. Alves ID, Jiao C-Y, Aubry S, Aussedat B, Burlina F, Chassaing G, Sagan S. Cell biology meets biophysics to unveil the different mechanisms of penetratin internalization in cells. Biochim Biophys Acta. 2010;1798(12):2231–2239.

33. Jahnsen RD, Sandberg-Schaal A, Vissing KJ, Nielsen HM, Frimodt-Møller N, Franzyk H. Tailoring Cytotoxicity of Antimicrobial Peptidomimetics with High Activity against Multidrug-Resistant Escherichia coli. J Med Chem. 2014;57(7):2864−2873.

34. Zhu WL, Shin SY. Antimicrobial and cytolytic activities and plausible mode of bactericidal action of the cell penetrating peptide penetratin and its lys-linked two-stranded peptide. Chem Biol Drug Des. 2009;73(2):209–215.

35. Alves ID, Goasdoué N, Correia I, Aubry S, Galanth C, Sagan S, Lavielle S, Chassaing G. Membrane interaction and perturbation mechanisms induced by two cationic cell penetrating peptides with distinct charge distribution. Biochim Biophys Acta. 2008;1780(7-8):948–959.

36. Palm C, Netzereab S, Hällbrink M. Quantitatively determined uptake of cell-penetrating peptides in non-mammalian cells with an evaluation of degradation and antimicrobial effects. Peptides. 2006;27(7):1710–1716.

37. Caesar CEB, Esbjörner EK, Lincoln P, Nordén B. Membrane interactions of cell-penetrating peptides probed by tryptophan fluorescence and dichroism techniques: correlations of structure to cellular uptake. Biochemistry. 2006;45(24):7682–7692.

38. Lindberg M, Jarvet J, Langel U, Gräslund A. Secondary structure and position of the cell-penetrating peptide transportan in SDS micelles as determined by NMR. Biochemistry. 2001;40(10):3141–3149.

39. Hein-Kristensen L, Knapp KM, Franzyk H, Gram L. Selectivity in the potentiation of antibacterial activity of α-peptide/β-peptoid peptidomimetics and antimicrobial peptides by human blood plasma. Res Microbiol. 2013;164(9):933–940.

40. Almeida PF. Membrane-active peptides: Binding, translocation, and flux in lipid vesicles. Biochim Biophys Acta. 2014;1–12.

Legend to figures

Figure 1 – Cellular uptake of three TAMRA labeled AMPs versus that of TAMRA-penetratin measured by flow cytometry in HeLa cells. Prior to analysis, the cells were incubated with 10 μM of each peptide for 1 hr at 37°C. The plot represents the mean of the medians of the raw data in triplicate error bars representing ±SD and normalized against the mean of penetratin. *P<0.05, **P<0.01, ***P<0.001 statistically significant differences.

Figure 2 - Cellular distribution of three selected AMPs (PK-12-KKP, SA-3, TPk) and penetratin (Pen) (all TAMRA labeled). For each photo montage: Left, grayscale: peptide; middle, grayscale: dextran/transferrin; right, red: peptide, green: transferrin/dextran, yellow: dextran/transferrin co-localized with peptide; blue: DRAQ7®. **Dextran**: The cells were incubated with 0.1 mg/mL dextran for 210 min and further incubated in media for 20 h before exposure to 10 μM peptide for 1 h (all at 37°C). **Transferrin**: The cells were incubated for 50 min with 100 nM transferrin and further incubated with both 100 nM transferrin and 10 μM of the peptides for 10 min (all at 37°C). Media for all samples contained 0.3 % (v/v) DRAQ7®. Images are representative single cross sections from the middle of cells. Scale bars correspond to 10 μm.

Figure 3 - Circular dichroism spectra of (a) PK-12-PPK; (b) SA-3; (c) TPk and (d) penetratin in TFE-water 90:10 (solid line) or in the presence of liposomes representing the membranes of Gram-positive bacteria, POPG:CL (3:1 molar ratio; dashed line); Gram-negative bacteria, POPG:CL:DOPE (2:7:1 molar ratio; dotted line); and eukaryotic cells, POPC:cholesterol (10:1 molar ratio; dashed and dotted line). Measurements were performed with a peptide concentration of 10 μM peptide to a lipid concentration of 1 mM yielding a peptide-to-lipid molar ratio of 1:100.

Figure 4 – Release of calcein from liposomes consisting of POPG:CL upon incubation with the antimicrobial peptide, SA-3, and the cell-penetrating peptide, penetratin. **Top:** Time-resolved release of calcein starting within 10 sec of peptide addition is depicted yellow: 0.1 μM; purple: 0.2μM; green: 0.4 μM; red: 0.8 μM and blue: 1.6

μM. **Bottom:** The relative release after 680 sec versus the total calcein entrapped. Each point represents the mean ±SD (n=3).

Table I. Amino acid sequences, number or residues and molecular weight of the investigated peptide variants.

Compound	Sequence	Residues	Mw	Ref
PK-12-KKP	KKPWWKPWWPKWKK-amide	14	2008.46	[15]
SA-3	IKWAGKWWKLFK-amide	12	1589.97	[16]
TPk	VRRFkWWWkFLRR-amide*	13	1963.38	[17]
Pen	RQIKIWFQNRRMKWKK-amide	16	2245.74	[18]
TAMRA-PK-12-KKP	TAMRA-KKPWWKPWWPKWKK-amide	14	2420.89	
TAMRA-SA-3	TAMRA-IKWAGKWWKLFK-amide	12	2002.40	
TAMRA-TPk	TAMRA-VRRFkWWWkFLRR-amide	13	2375.81	
TAMRA-Pen	TAMRA-RQIKIWFQNRRMKWKK-amide	16	2658.17	

*k refers to NLys [H_2N-$(CH_2)_4$-NH-CH_2-COOH].

Table II – Viability of mammalian cells and minimal inhibitory concentrations

	Eukaryotic cell viability[a]			MIC (μM)	
	NIH 3T3	HUVEC	HeLa WT	*S. aureus*[b]	*E. coli*[c]
PK-12-KKP	>256	>256	>256	32	16-32
SA-3	30 ± 4.5	128-256[#]	27 ± 1.7	32	16-32
TPk	128-256[#]	>256	41 ± 4.0	8-16	2
Pen	>256	>256	>256	32	8-16

[a] EC_{50} values are given in μM (n=3 in 3 passages; mean±SD) as the concentration required to give a 50% reduction in viability of the cells after incubation with peptide for 1 h. [#] EC_{50} listed as an interval as the value was too close to the maximum concentration to allow accurate fitting.
[b] Strain: ATCC 25923. [c] Strain: ATCC 25922.

Table III – Maximum calcein release after exposure to a concentration of 1.6 μM peptide expressed as percent of total amount of calcein released (mean± SD).

	POPG:CL (3:1)[a] *S. aureus* model	POPG:CL:DOPE (2:7:1)[b] *E. coli* model	POPC:cholesterol (10:1)[c] Eukaryotic model
PK-12-PPK	23.6 ± 6.1*	13.1 ± 1.7	24.3 ± 2.4
SA-3	82.2 ± 1.4	101.7 ± 1.7	33.2 ± 2.2
TPk	32.5 ± 1.3	2.7 ± 0.5	36.6 ± 4.5
Pen	99.6 ± 0.6	13.3 ± 1.4	8.4 ± 0.8

[a] *S. aureus* membrane model, (n=3) [b] *E. coli* membrane model, (n=2), [c] Eukaryotic membrane model (n=3). Run time 680 sec; *Run time 340 sec.

Figure 1

Click here to download high resolution image

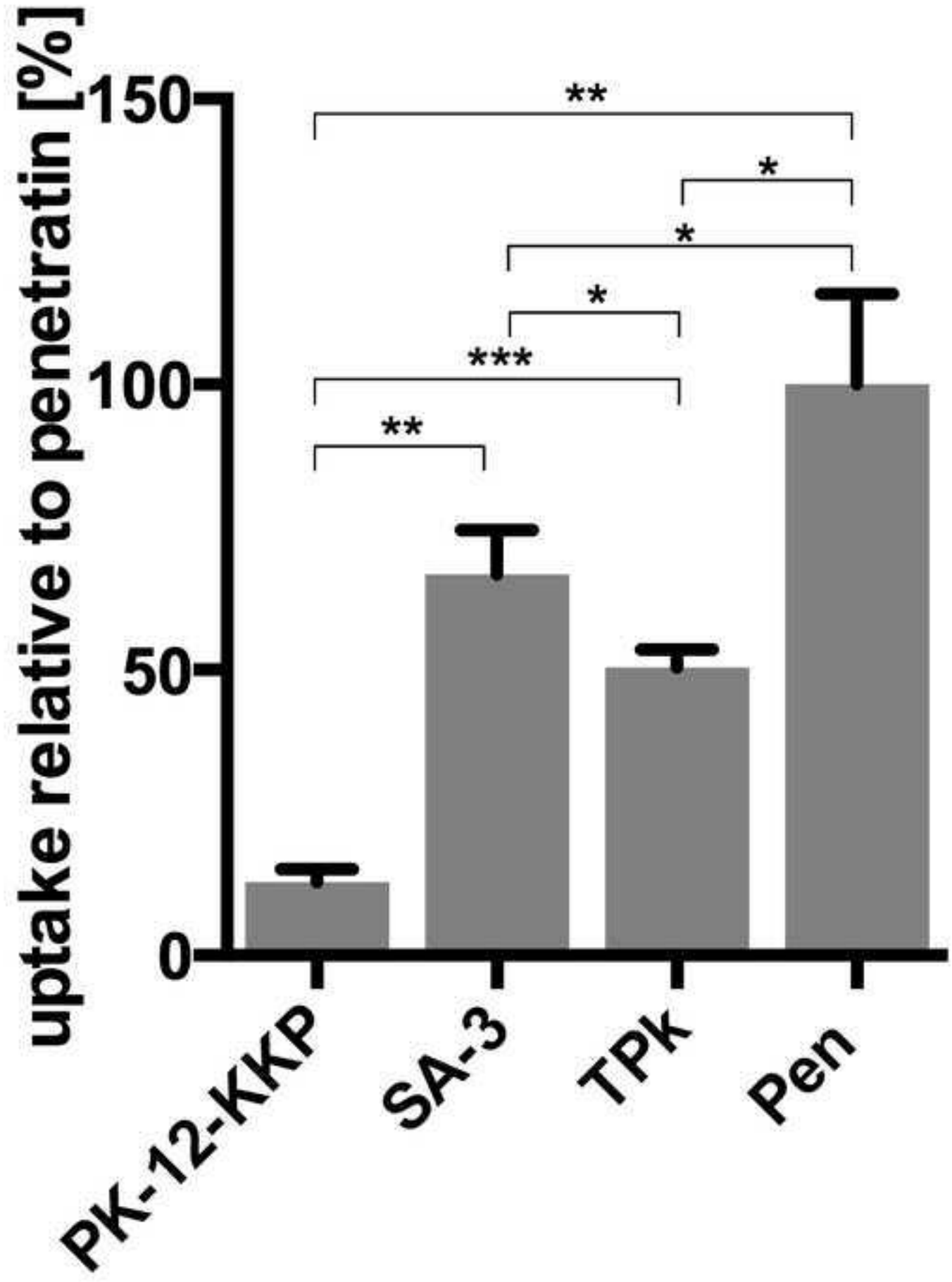

Figure 2
Click here to download high resolution image

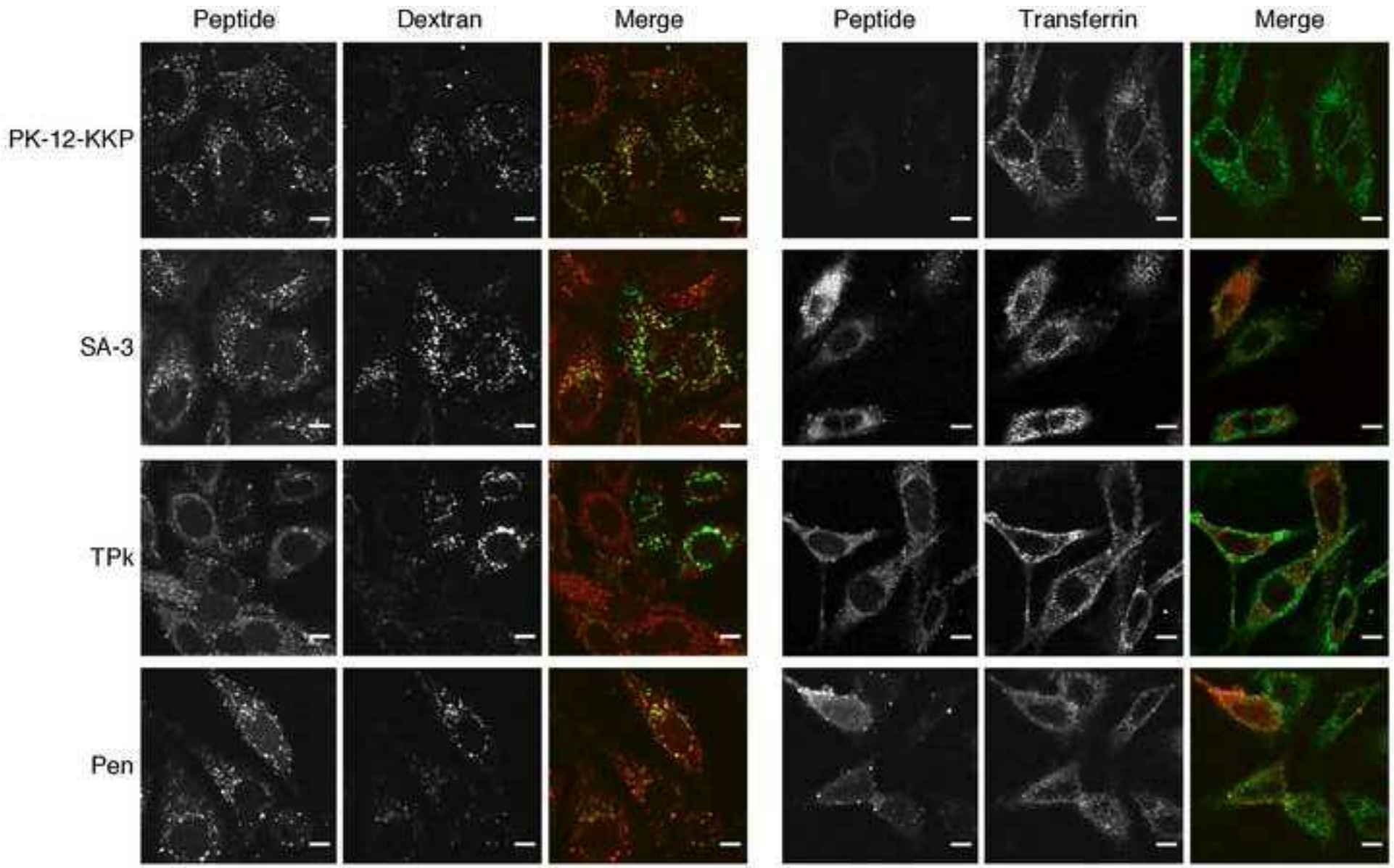

Figure 3
Click here to download high resolution image

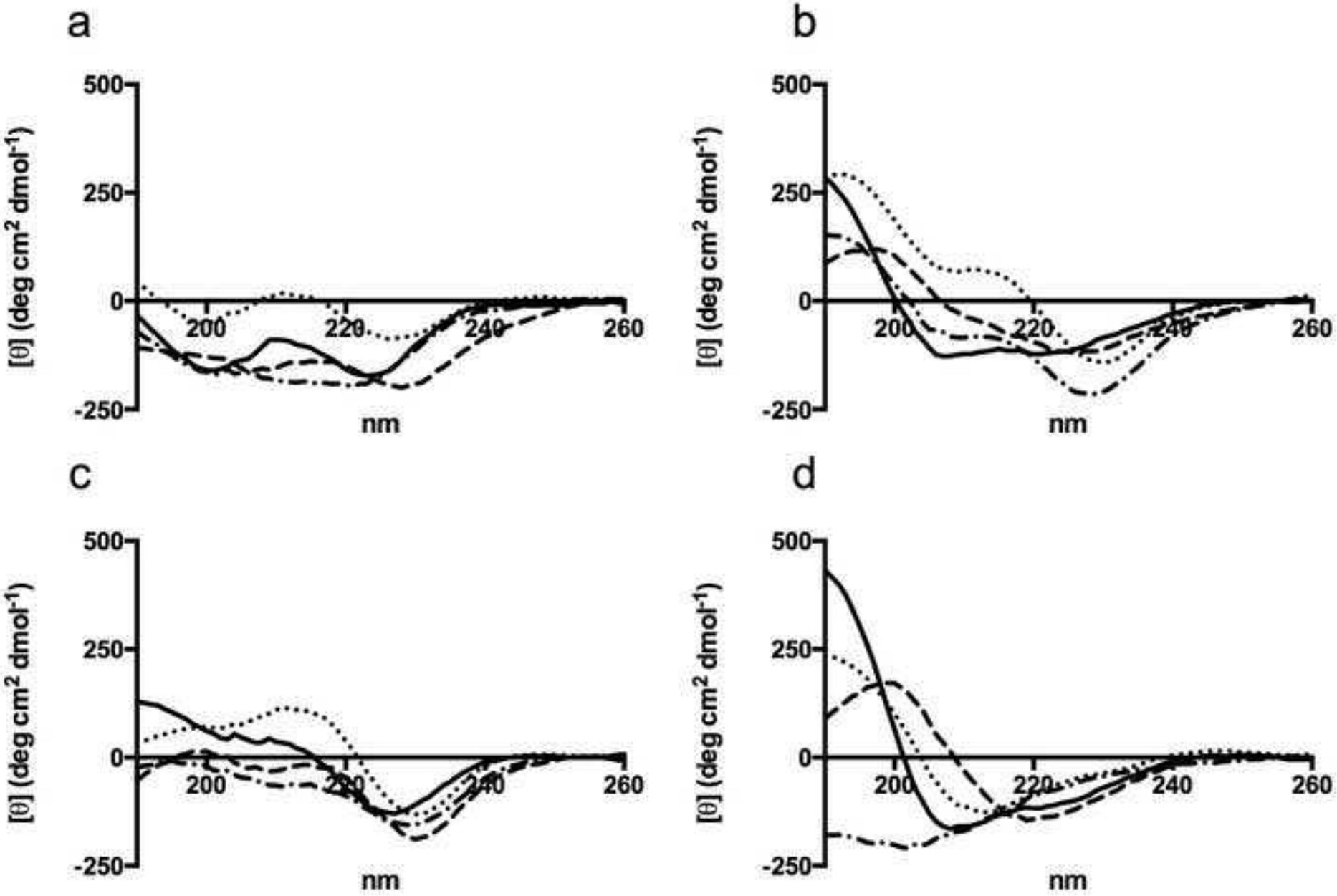

Figure 4
Click here to download high resolution image